Analysis and optimization of the performance of the electro-optic technique used for ultrashort relativistic electron bunches

Kun Meng (孟 坤)*, Zeren Li (李泽仁), and Qiao Liu (刘 乔)

Institute of Fluid Physics, China Academy of Engineering Physics, Mianyang 621900, China

**Corresponding author: mengkunsdu@yahoo.com.cn*

Received December 15, 2010; accepted January 22, 2011; posted online June 27, 2011

The electro-optic (EO) technique used in the terahertz spectral technology is described. Response functions—which are used to describe the EO detecting efficiency—of five types of cubic EO crystals are calculated. Based on these results, the choice of different crystal thicknesses is discussed. In the EO detecting procedure, certain factors, such as reflection, dispersion, absorption and velocity mismatch, may distort the temporal profile of the electric field being detected; therefore, these factors are calculated. The relationship between the field distortion and the bunch duration as well as the crystal thickness is considered.

OCIS codes: 260.3090, 300.6495, 260.2065, 280.4991.
doi: 10.3788/COL201109.S10206.

Dense, relativistic electron bunches for picosecond or sub-picosecond durations are important elements for several advanced accelerators, which are employed in linear electron-positron colliders, X-ray free electron laser, etc. Precise measurement of the temporal profile of these electron bunches is essential for monitoring and operating the accelerators, as well as for understanding the physical processes active in these accelerators.

The single-shot electro-optic (EO) method, which was first demonstrated by Jiang *et al.*[1], is a promising method for obtaining the temporal profile of ultrashort electron bunches[2−5] because of its real-time and non-destructive properties. This method is based on the fact that the local electric field of a relativistic electron bunch moving in a straight line within a vacuum is almost entirely perpendicular to the direction of motion[6]. Therefore, the width of the temporal profile of the electric field corresponds directly to the length of the electron bunch; the shape of the temporal profile is proportional to the longitudinal electron distribution within the electron bunch. The electric field is equivalent to a half-cycle terahertz (THz) pulse, which can induce birefringence in the EO crystal located in the vicinity. The transmission of a chirped laser-pulse through the crystal, synchronously with the electron bunch, results in the "coding" of the electric field of the bunch on the laser-pulse. A comparison of the laser-pulse obtained, both with and without the electron bunch, can help obtain the temporal profile of the bunch.

By using this method, the distortion of the THz wave traveling through the EO crystal should be considered primarily; this is because the distortion may affect the accuracy of the measurement and restrict the range of its application.

In this letter, we describe the EO technique used in the THz spectral technology. Further, the response functions of five different types of usual cubic EO crystal materials are calculated and the relationships between the thickness of the crystal and the frequency that is bound to be detected are discussed. Thereafter, the distortion of the electric field and the temporal profile detected for the electric field, with regard to the velocity mismatch between the electric field and the probe laser pulse, are calculated. The effect of the time length of the electron bunch and the results of detection with different retardations between the chirp probe laser pulse and the electron bunch are also calculated.

The EO measurement method was developed based on the linear EO effect (Pockel's effect). The incident THz wave can modify the refractive index ellipsoid of the EO crystal. When a probe pulse traverses the crystal, it becomes modulated. Three methods can detect the modulation effect, that is, phase modulation detection[7], amplifier modulation detection[8], and polarization modulation detection[9]. By comparing modulations effected both with and without the THz wave, the form of the THz pulse can be obtained.

For real-time measurement, the single-shot detection technique is recommended. When using a grating pair to chirp the fs pulse, the THz pulse can be coded by one probe pulse[6]; that is, the THz waveform can be obtained by a single shot.

To obtain quantitative EO detecting efficiency impacted by velocity mismatch, the response function is defined as[10]

$$G(f,d) = \frac{2}{1+n(f)+\mathrm{i}\kappa(f)}\frac{1}{d} \times \int_0^d \exp\{\mathrm{i}2\pi f z[\frac{1}{\nu_{\mathrm{ph}}(f)} - \frac{1}{\nu_{\mathrm{g}}}]\}\mathrm{d}z, \quad (1)$$

where $n(f)+\mathrm{i}\kappa(f)$ is the frequency-dependent complex refractive index, $\nu_{\mathrm{ph}}(f)$ is the phase velocity of the THz wave, ν_{g} is the group velocity of the probe pulse, d is the thickness of the crystal, f is the frequency of the THZ wave, and z is the traveling distance of the THZ wave.

Five cubic crystal materials, ZnTe, GaP, InP, GaAs, and ZnS, have the potential to be used as the detecting

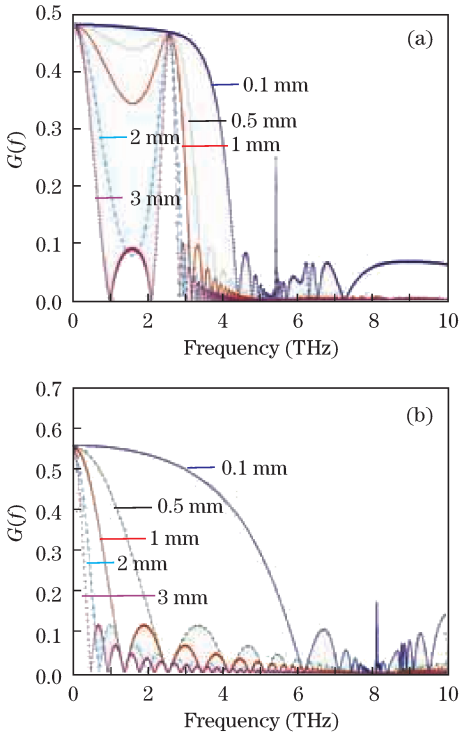

Fig. 1. Response functions of crystals with different thicknesses. (a) ZnTe; (b) ZnS.

EO crystal. By using the data provided by Refs. [10,11], the response functions of crystals with different thicknesses can be calculated. Some results are shown in Fig. 1.

Figure 1(a) presents curves of ZnTe in which the probe pulse and some of the detected THz waves have the same transmission speed; a similar situation exists in GaP and GaAs. Figure 1(b) shows the curves of ZnS in which the probe pulse is shown to constantly travel faster than the THz wave; a similar phenomenon has been observed to exist in InP.

Similar results to that shown in Fig. 1(a) can be found in other published reports[10]. From this figure, the zero point for all thicknesses can be observed; this is called the transverse optical (TO) lattice oscillation frequency of the EO crystal. Further, it is identified that there exists a trough between two main peaks of the response function curve; as the thickness of the crystal increases, the trough will reduce until it reaches a value of zero, after which it "rebounds". The first main peak is the zero-frequency point, and the second main peak is the velocity matching point. The trough is caused by the velocity mismatch. With the increase in thickness, the mismatch increases as well, and this induces the response function to decrease. When the response function becomes zero, the mismatch is equal to $(n + 1/2)\lambda$.

When the response function becomes zero for the first time, with the increase in the thickness of the crystal, the crystal is deemed to have become unusable; this is because it is incapable of reconstructing the detected waveform. Therefore, the maximum thickness of the crystal as a detector can be calculated. In addition, it is notable that the response function contains a coefficient $1/d$, and the EO detecting sensitivity is proportional to $G \times d$. With regard to this factor, the optimum thickness of the crystal can be calculated to provide detection with the highest sensitivity. The results are shown in Table 1.

The velocity match cannot be satisfied in InP and ZnS when the wavelength of the probe pulse is 800 nm. The frequency bound of these crystals for detection is considered to decrease with the increase in thickness, as shown in Fig. 1(b). The relation between the frequency bound and the thickness of the crystal is calculated and shown in Fig. 2.

Certain factors, such as reflection, dispersion, and absorption[10,12], may cause distortion of the THz wave when it travels through the crystal. A further distortion of the detected THz waveform will be factored in for the velocity mismatch between the THz pulse and the probe pulse. These distortions, as a consequence, affect the accuracy of measurement of the electron bunch. These waveform distortions have been calculated. The electron bunch longitudinal charge distribution has been taken as[10]

$$\rho(z,t) = \frac{Q}{\sqrt{2\pi}c\sigma_t} \exp\left[-\frac{(z-ct)^2}{2c^2\sigma_t^2}\right], \qquad (2)$$

where Q is the electron bunch power, z is the coordinate, c is the speed of light, and t is the time. The longitudinal charge distribution in the electron bunch is described by a Gaussian of variance, $\sigma_z = c\sigma_t$.

The reflection distorts the waveform mainly because the frequency-dependent reflection causes different losses of various frequency components at the interface. The dispersion and absorption are caused by the real and imaginary parts of the refractive index, respectively. In addition, these can cause frequency-dependent phase change and decrease in intensity that result in distortion of the waveform. The velocity mismatch will affect the detecting efficiency of different frequency components of the THz wave.

By considering the reflection, dispersion, and absorption altogether, the distorted waveform of the THz pulse traveling through the crystal is obtained. On the interior, the detected waveform is also calculated by taking

Table 1. Calculation Results of the Maximum and the Optimum Thicknesses of ZnTe, GaP, and GaAs

	ZnTe	GaP	GaAs
Maximum Thickness (mm)	2.34	0.24	8.07
Optimum Thickness (mm)	1.82	0.12	4.02

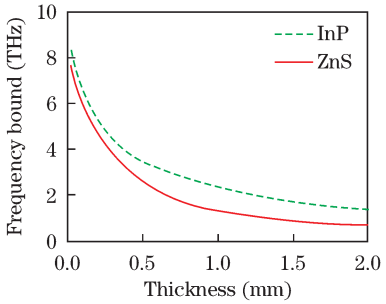

Fig. 2. Relationship between the frequency bound and the crystal thickness.

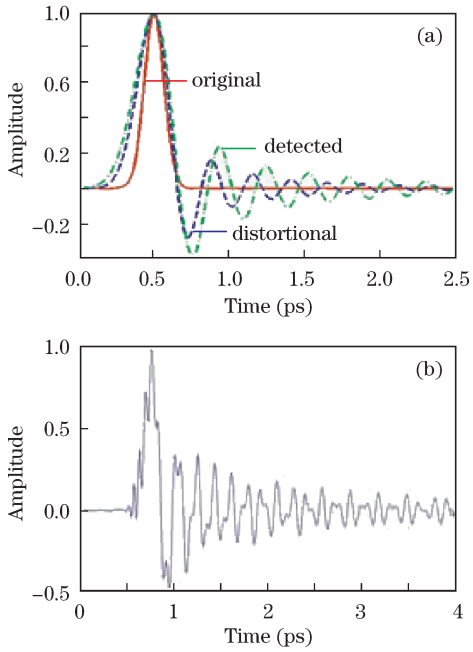

Fig. 3. Distortion of the waveform.

the velocity mismatch into account. The results obtained in this study are shown in Fig. 3(a).

Figure 3(a) demonstrates that the THz wave may become broad and develop apparent oscillations in the tail of the curve during the process of propagation and detection. As the electron bunch becomes shorter, the distortion may become more severe until the appropriate form of the bunch is obtained. Figure 3(b) presents an example of a situation with extreme distortion, which is the result detected for a 20-fs electron bunch by a 100-μm GaAs.

The broadening at the full-width at half-maximum (FWHM) is used to estimate the distortion of the waveform when it is not severely distorted. The broadening of the electric field of different durations of electron bunches is calculated. The results obtained for five different crystals are shown in Fig. 4(a). It indicates that when the wave becomes shorter, the distortion may become so great that one cannot obtain the real form of the electron bunch: this indicates the limitation of the detected resolving power.

As shown in Fig. 4(a), for the short electron bunch, the crystal with a higher TO frequency manifests superiority as a detector; examples of these include GaP and ZnS. This is because, with a shorter wave, the higher the frequency of the components it contains. Further, the thickness of the crystal affects the resolving power, and certain calculation results are shown in Fig. 4(b).

In conclusion, by using the experimental material data provided in the handbook, the response function of five EO crystals are calculated. The optimum thickness of ZnTe, GaP, and GaAs are deduced to be 1.82, 0.12, and 4.02 mm, respectively, and their maximum available thicknesses are 2.34, 0.24, and 8.07 mm, respectively. For InP and ZnS, their detecting frequency bounds decrease with the increase in their thickness. Then, the quantity relationship between waveform distortion and the duration of electron bunch, as well as crystal thickness, are

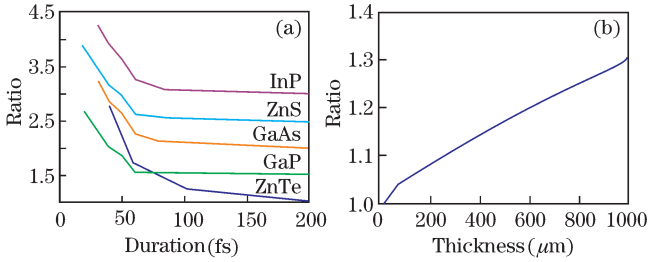

Fig. 4. (a) Electron bunch duration versus the ratio of the FWHM between the detected and original wave, and the vertical zero is offset for each trace by 0.5; (b) Thickness of the GaP versus the ratio of the FWHM between the detected and original wave.

derived and provided. These results indicate that the distortion becomes more severe as the electron bunch gets shorter and the crystal gains thickness. These results facilitate selection of type and symmetry of the EO crystal that is to be used as a detector to measure the electron bunch, or for other purposes that require THz detection. The finding in this letter also help the estimation of the detected results.

This work was supported by the Science and Technology Development Fund of China Academy of Engineering Physics under Grant No. 2008B0403038.

References

1. Z. Jiang and X.-C. Zhang, Appl. Phys. Lett. **16,** 1945 (1998).
2. I. Wilke, A. M. Macleod, W. A. Gillespie, G. Berden, G. M. H. Knippels, and A. F. G. van der Meer, Phys. Rev. Lett. **12,** 124801 (2002).
3. G. Berden, S. P. Jamison, A. M. Macleod, W. A. Gillespie, B. Redlich, and A. F. G. van der Meer, Phys. Rev. Lett. **11,** 124802 (2004).
4. G. Berden, W. A. Gillespie, S. P. Jamison, E.-A. Macleod, A. M. Macleod, A. F. G. van der Meer, P. J. Phillips, H. Schlarb, B. Schmidt, P. Schmuser, and B. Steffen, Phys. Rev. Lett. **99,** 164801 (2007).
5. A. D. Debus, M. Bussmann, U. Schramm, R. Sauerbrey, C. D. Murphy, Zs. Major, R. Hörlein, L. Veisz, K. Schmid, J. Schreiber, K. Witte, S. P. Jamison, J. G. Gallacher, D. A. Jaroszynski, M. C. Kaluza, B. Hidding, S. Kiselev, R. Heathcote, P. S. Foster, D. Neely, E. J. Divall, C. J. Hooker, J. M. Smith, K. Ertel, A. J. Langley, P. Norreys, J. L. Collier, and S. Karsch, Phys. Rev. Lett. **104,** 084802 (2010).
6. J. D. Jackson, *Classical Electrodynamics* (Wiley, New York, 1975).
7. J. Latess, C. J. Lazard, S. Sriram, and S. A. Kingsley, Proc. SPIE **3158,** 79 (1997).
8. P. O. Muller, S. B. Alleston, A. J. Vickers, and D. Erasme, IEEE J. Quantum Electron. **1,** 7 (1999).
9. L. Duvillaret, S. Rialland, and J.-L. Coutaz, J. Opt. Soc. Am. B **11,** 2704 (2002).
10. S. Casalbuoni, H. Schlarb, B. Schmidt, P. Schmuser, B. Steffen, and A. Winter, TESLA Report 2005-01.
11. E. D. Palik, *Handbook of Optical Constants of Solids* (Academic Press, San Diego, 1985).
12. H. J. Bakker, G. C. Cho, H. Kurz, Q. Wu, and X.-C. Zhang, J. Opt. Soc. Am. B **6,** 1795 (1998).